Solar wind spectral analysis in heliosheath from Voyager 2 data

F. Fraternale[1], L. Gallana[1], M. Iovieno[1], E. Magli[2], S.M. Fosson[2], M. Opher[3], J.D. Richardson[4], D. Tordella[1]

[1] *Department of Mechanical and Aerospace Engineering Politecnico di Torino*
[2] *Department of Electronics and Telecommunications Politecnico di Torino*
[3] *Astronomy Department, Boston University*
[4] *Kavli Institute for Astrophysics and Space Research, Massachusetts Institute of Technology*

European Turbulence Conference 2015
Delft, 25-28 August 2015

Aims

Performing a reliable spectral analysis on gapped Heliosheath data, with focus on turbulence

Analyzing differences between unipolar and sectored heliosheath from a spectral point of view

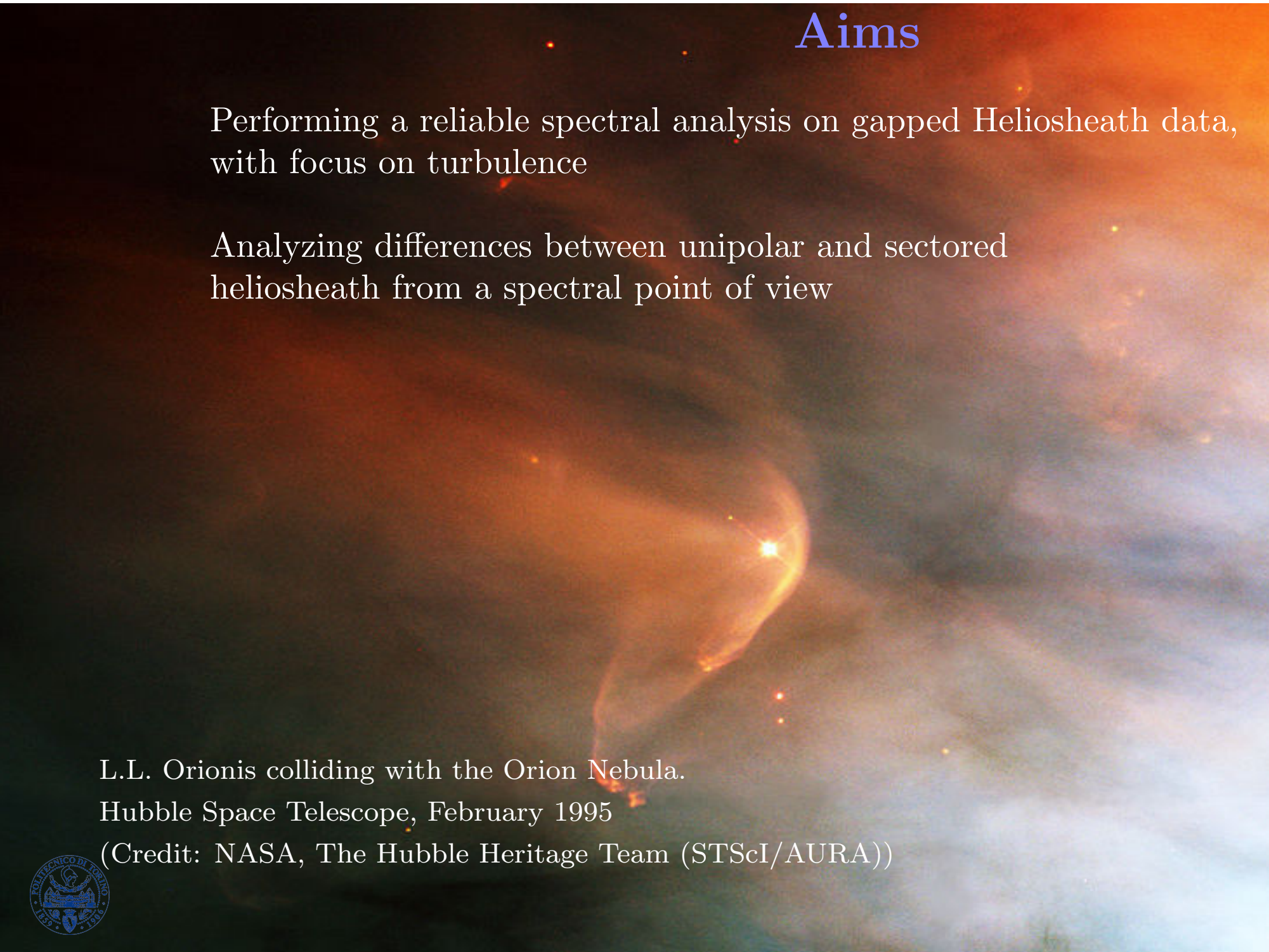

L.L. Orionis colliding with the Orion Nebula.
Hubble Space Telescope, February 1995
(Credit: NASA, The Hubble Heritage Team (STScI/AURA))

Voyager 2 Interstellar Mission

- *Voyager 2* is flying now at 15.5 km/s, 107.84 *AU* from Earth, in the *Heliosheath*, the outermost layer of the heliosphere where the solar wind is slowed by the pressure of interstellar gas
- *Termination Shock* was passed on Sep 5, 2007 at 84 AU

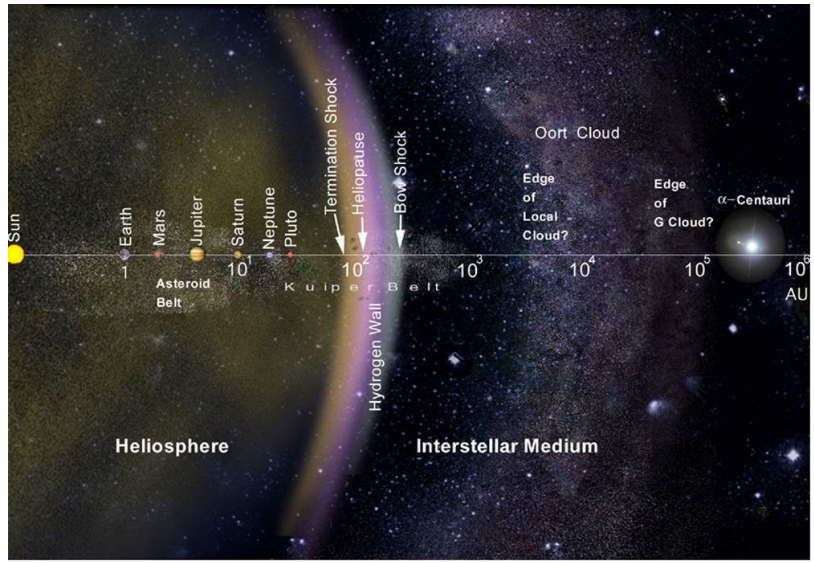

source: http://voyager.jpl.nasa.gov

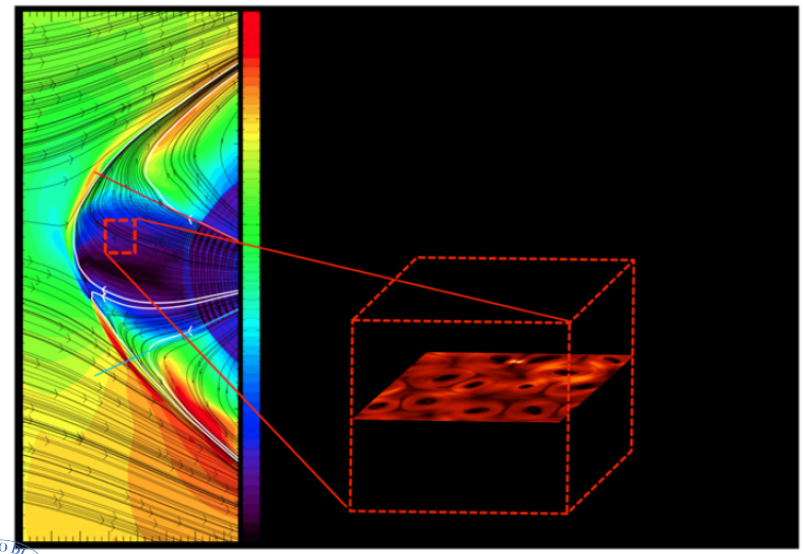

source: M. Opher et al.

A turbulence hypothesis for the magnetic field in the *Heliosheath*
M. Opher et al, ApJ 734, 2011
"*Is the magnetic field in the Heliosheath laminar or a turbulent sea of bubbles?*"

The Heliosheath

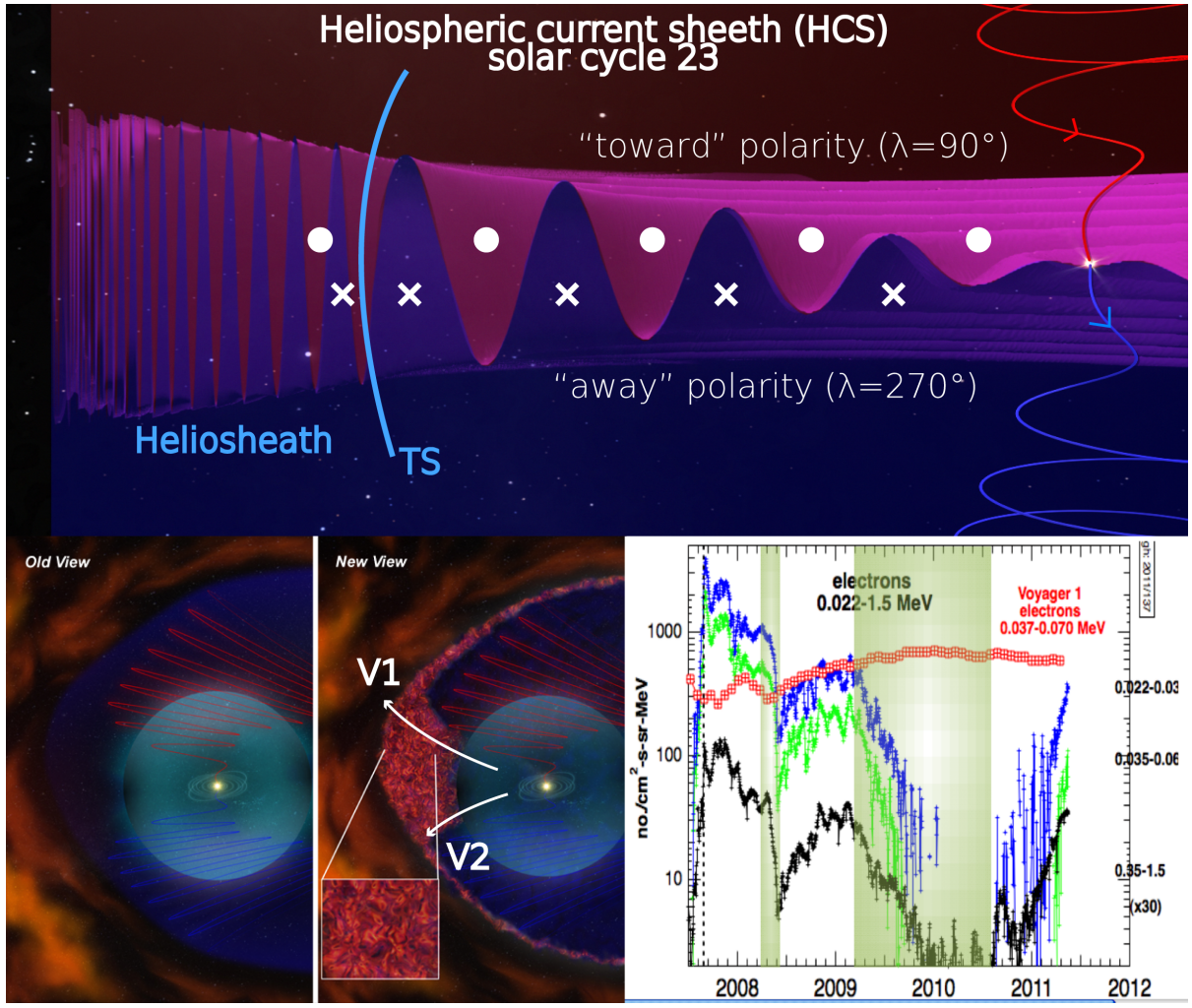

- At the termination shock (TS) the plasma slows to subsonic regime and is compressed, so the density, temperature, and magnetic field magnitude all increase
- The sector spacing decreases after the Termination Shock to about 2AU. Magnetic reconnection is triggered close to HP and the sectors break up into magnetic islands (bubbles), convected with the flow [Opher et al ApJ, 2011]. → magnetic islands/ bubbles can act as local traps for energetic electrons.
- Is there a change in the nature of turbulence in the heliosheath?

Unipolar and sectored heliosheath

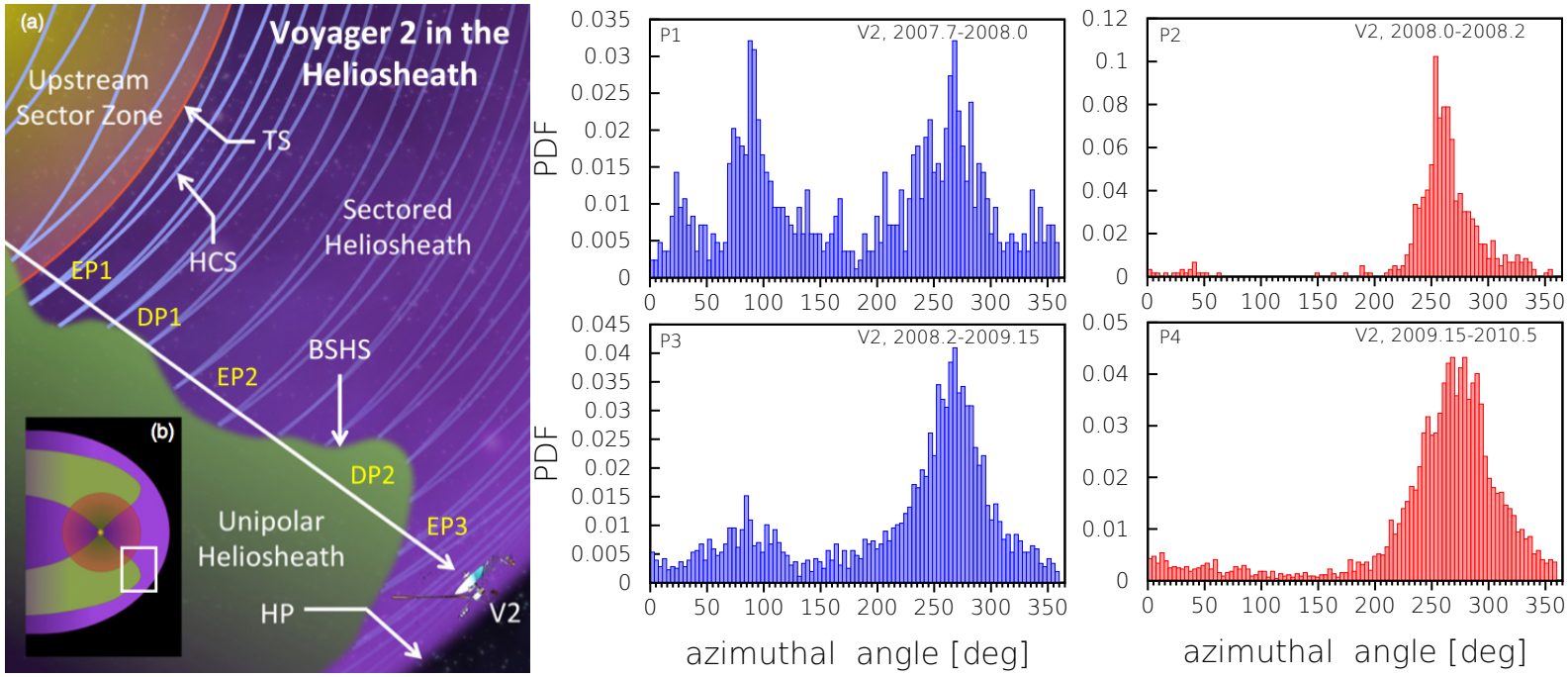

Four periods are identified:

- **P1** 2007.7 - 2008.0 - Sectored Heliosheath (SH)
- **P2** 2008.0 - 2008.2 - Unipolar Heliosheath (UH)
- **P3** 2008.2 - 2009.15 - Sectored Heliosheath (SH)
- **P4** 2009.15 - 2010.5 Unipolar Heliosheath (UH)
- 2011 Unipolar Heliosheath (UH) (effects of solar minimum of 2009 - [Burlaga et at. 2011 JGR])

Field and plasma data

9/2007- 6/2010 → Heliosheath, 84-94 AU

	P1 (SH)	P2 (UH)	P3 (SH)	P4 (UH)	**Total**
$\langle \mathbf{n_i} \rangle$ $[dm^{-3}]$	2.16	1.71	1.17	1.14	**1.38**
$\mathbf{E}_k$ $[km^2/s^2]$	1511.8	1365.4	2210.1	1626.0	**1943.8**
$\mathbf{E}_m$ $[km^2/s^2]$	2498.7	1527.4	2226.0	1376.4	**1894.7**
$\langle \mathbf{V} \rangle$ $[km/s]$	153.2	159.2	164.0	143.7	**152.3**
$\langle \mathbf{V}_A \rangle$ $[km/s]$	65.7	52.3	60.25	58.9	**60.2**
$\langle \mathbf{B} \rangle$ $[nT]$	0.123	0.154	0.088	0.086	**0.095**
$\langle \mathbf{T} \rangle$ $[10^5 K]$	1.54	1.67	0.96	0.55	**0.98**
$\mathbf{c}_s$ $[km/s]$	1021.4	1119.2	997.7	803.6	**928.5**
β	2.43	3.59	1.36	0.69	**1.48**
$\mathbf{f}_{pi}$ $[Hz]$	9.05	8.53	7.08	6.98	**7.62**
$\mathbf{f}_{ci}$ $[Hz]$	0.0018	0.0014	0.0013	0.0013	**0.0014**
$\mathbf{f}_*$ $[Hz]$	0.037	0.029	0.041	0.046	**0.040**
$\mathbf{r}_i$ $[km]$	5542	5812	6975	7043	**6576**
$\mathbf{r}_{ci}$ $[km]$	4142	5517	4037	3138	**3778**
λ_D $[m]$	60.2	65.9	58.8	47.3	**54.7**

Spectral estimation techniques

70% of data are missing for hourly averages in the period 2007/2010 (**97%** for high resolution data). Reconstruction techniques are used in order to perform spectral analysis.

- Correlation spectral analysis
  Trace of the spectral correlation matrix after linear data interpolation
- Maximum likelihood reconstruction
  Statistical recovery constrained by data[1], improves the method of correlations.
- Compressed Sensing - Basis Pursuite DeNoise (CS-BPDN)
  Recently introduced in telecommunication[2]. Reconstruction of signal from sparse (compressed) dataset.
- Optimization method (via genetic algorithm)
  A model piecewise linear spectrum converges to the solution via an optimization process. [3].

[1] Rybicki & Press, ApJ 398, 1992
[2] Donoho, IEEE TIT, 2006
[3] Koza, *Genetic programming*, MIT Press Cambridge 1992

Synthetic sets with 30% of missing data

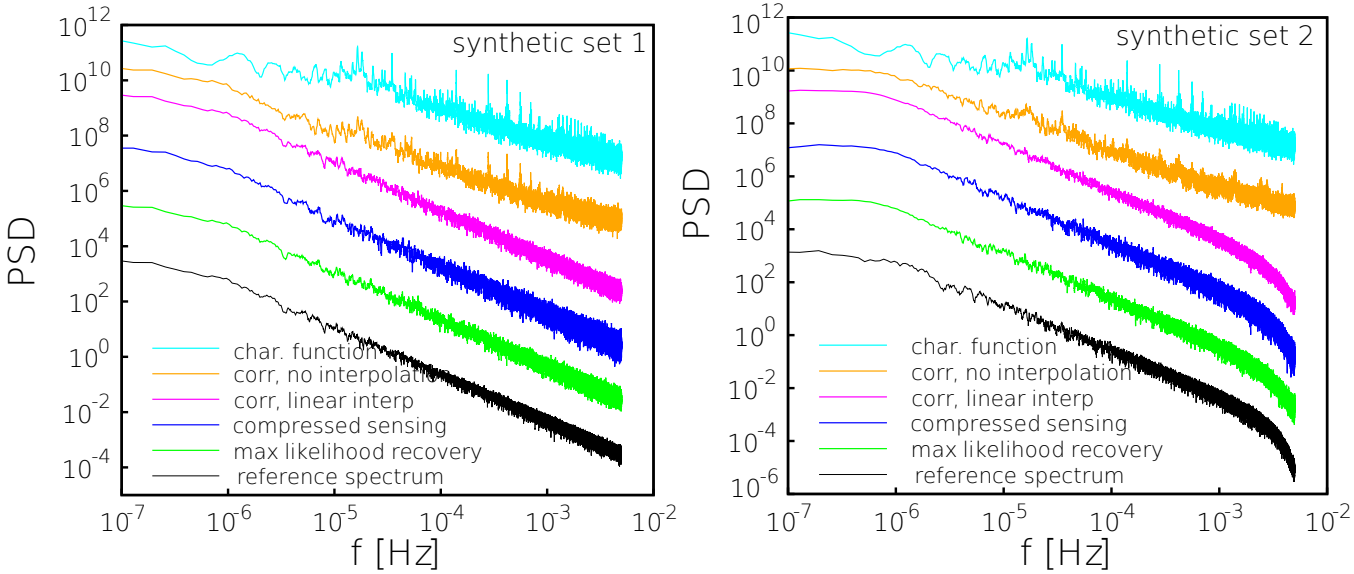

- set 1$\rightarrow$ $E_{3D}(n/n_0) = \frac{(n/n_0)^{\beta}}{1+(n/n_0)^{\alpha+\beta}}$
- set 2 $\rightarrow$ $E_{3D}(n/n_0) = \frac{(n/n_0)^{\beta}}{1+(n/n_0)^{\alpha+\beta}} * \left[1 - exp(\frac{n-n_{tot}}{\gamma} + \epsilon)\right]$

$$n = 1, ..., ntot/2 \quad f(n) = n/T$$

E_{1D} is obtained integrating the formula: $E_{3D}(f) = -f dE_{1D}/df$

$$\beta = 2,\ \alpha = 5/3,\ n_0 = 11,\ \gamma = 10^4,\ \epsilon = 10^{-1}$$

- Synthetic data are scaled on a 180 days time grid ($\Delta t = 100\ s$, $n_{tot} = 155520$)
- The same gaps of V2 velocity data are projected on these sequences

Synthetic sets with 70% of missing data

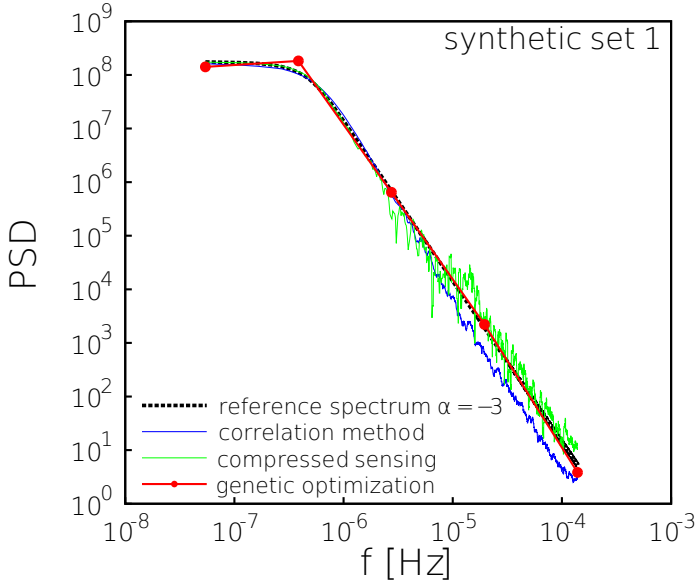

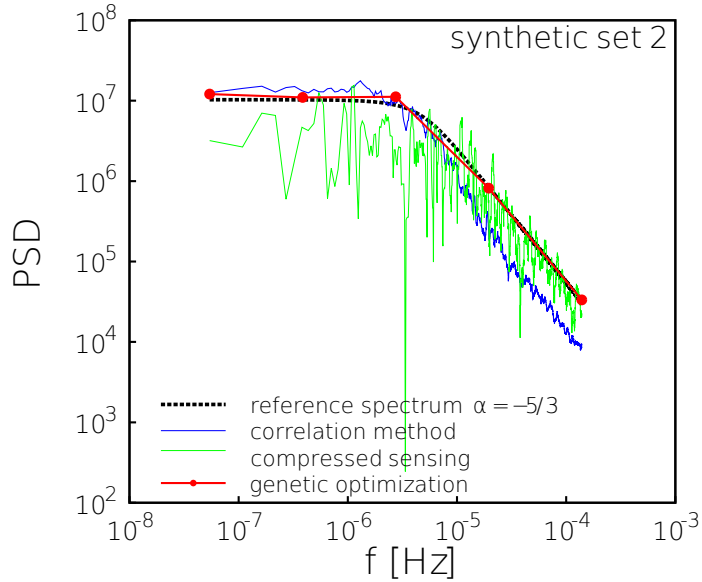

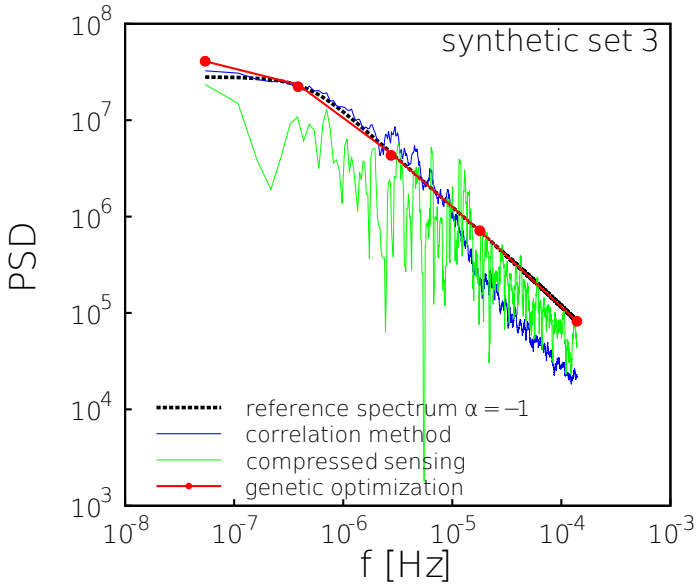

Hourly data ($\Delta t = 3600$ s, $n_{tot} = 5120$). Same gaps of V2 magnetic field in 2011 (missing data 70%).

$E_{3D}(n/n_0) = \frac{(n/n_0)^{\beta}}{1+(n/n_0)^{\alpha+\beta}}$

- set 1 $\rightarrow \beta = 2$, $\alpha = 3$, $k_0 = 10$
- set 2 $\rightarrow \beta = 2$, $\alpha = 5/3$, $k_0 = 100$
- set 3 $\rightarrow \beta = 2$, $\alpha = 1$, $k_0 = 10$

Heliosheath velocity field

Analysis 2007.7–2010.5 (AU- AU)

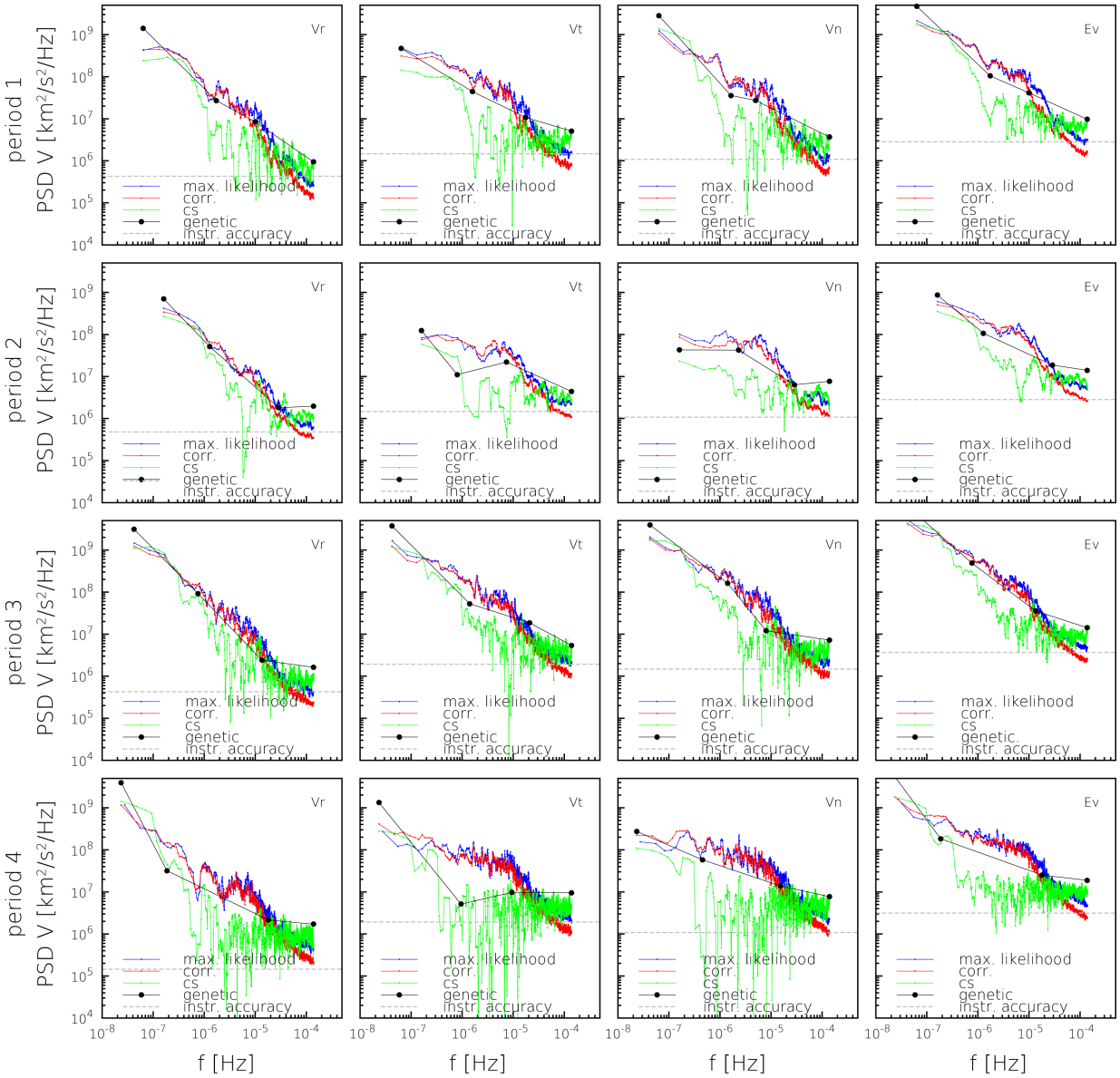

Heliosheath magnetic field

Analysis 2007.7–2010.5

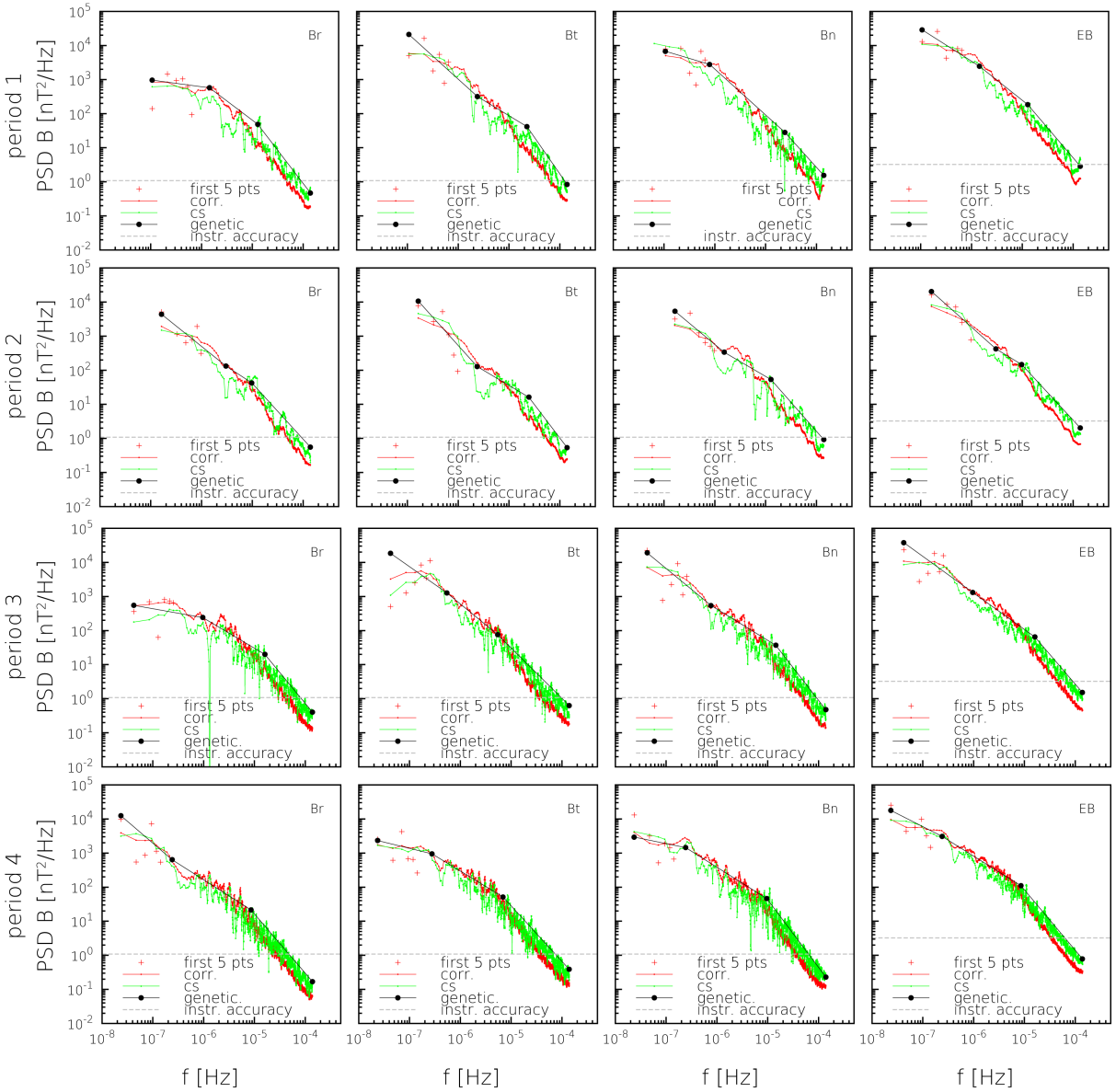

Spectral power laws
magnetic field

In the tables the scaling exponents are shown. The spectra are fit to a power law $E(f) \approx f^{\alpha}$ in two frequency ranges.

frequency range: $f < 10^{-5}$ (fit from corr. method)

period	B_R	B_T	B_N	$\|B\|$
P1	-0.91	-1.40	-1.36	-1.30
P2	-1.38	-1.33	-1.30	-1.33
P3	-1.00	-1.19	-1.11	-1.13
P4	-1.20	-1.16	-1.09	-1.13

frequency range: $f > 10^{-5}$ (fit from iterative method/ CS)

period	B_R	B_T	B_N	$\|B\|$
P1	-1.83	-1.91	-1.66	-1.74
P2	-1.63	-1.92	-1.69	-1.70
P3	-1.62	-1.60	-1.83	-1.74
P4	-1.73	-1.63	-1.85	-1.77

- Big scales: scaling exponents around unity
- A change in slope occurs at $f \approx 10^{-5}$ Hz
- For $f > 10^{-5}$ Hz the slope is higher than the Kolmogorov one

Scales of turbulence

magnetic field

In the tables the Integral scale (T) and the Taylor micro-scale (τ) are shown.

$$T_i = \frac{1}{\sigma_{B_i}} \sum_f \frac{\hat{B}_i^2}{f} \qquad \tau_i = \frac{1}{\sqrt{\sum_f f^2 \hat{B}_i^2 / \sigma_{B_i}}} \qquad \textit{Batchelor}, 1970$$

Integral scale [days / AU]

period	B_R	B_T	B_N	$\|B\|$
P1	12.6 / 1.11	28.9 / 2.55	27.6 / 2.43	25.8 / 2.27
P2	29.5 / 2.60	34.4 / 3.03	37.5 / 3.31	28.8 / 2.54
P3	23.5 / 2.22	43.1 / 4.07	50.7 / 4.79	55.3 / 6.74
P4	130 / 10.8	47.2 / 3.91	32.2 / 2.67	86.9 / 7.21
2007.7-2012.0	142 / 12.3	106 / 9.21	113 / 9.81	137 / 11.9

Taylor micro-scale [hrs/ AU]

period	B_R	B_T	B_N	$\|B\|$
P1	$8 / 2.94{\cdot}10^{-2}$	$10 / 3.67{\cdot}10^{-2}$	$16 / 5.87{\cdot}10^{-2}$	$11 / 4.04{\cdot}10^{-2}$
P2	$10 / 3.69{\cdot}10^{-2}$	$11 / 4.16{\cdot}10^{-2}$	$8 / 2.98{\cdot}10^{-2}$	$9 / 3.30{\cdot}10^{-2}$
P3	$8 / 3.14{\cdot}10^{-2}$	$16 / 6.30{\cdot}10^{-2}$	$10 / 3.93{\cdot}10^{-2}$	$11 / 4.33{\cdot}10^{-2}$
P4	$11 / 3.80{\cdot}10^{-2}$	$12 / 4.14{\cdot}10^{-2}$	$13 / 4.49{\cdot}10^{-2}$	$12 / 4.14{\cdot}10^{-2}$
2007.7-2012.0	$10 / 3.60{\cdot}10^{-2}$	$13 / 4.68{\cdot}10^{-2}$	$13 / 4.68{\cdot}10^{-2}$	$12 / 4.32{\cdot}10^{-2}$

- Big scales: T increases as distance from the sun, P1 and P2 still show influence of solar rotation, later periods show dominant periodicities of about 100 days.
- [Opher et al. ApJ 2011]: Sector spacing is estimated to be about 2 AU in the HS, as well as the bubbles size.

Heliosheath, V2 and V1

Magnetic energy spectra

V2 crossed the TS in Aug. 2007 (84 AU), V1 in Dec. 2004 (94 AU)

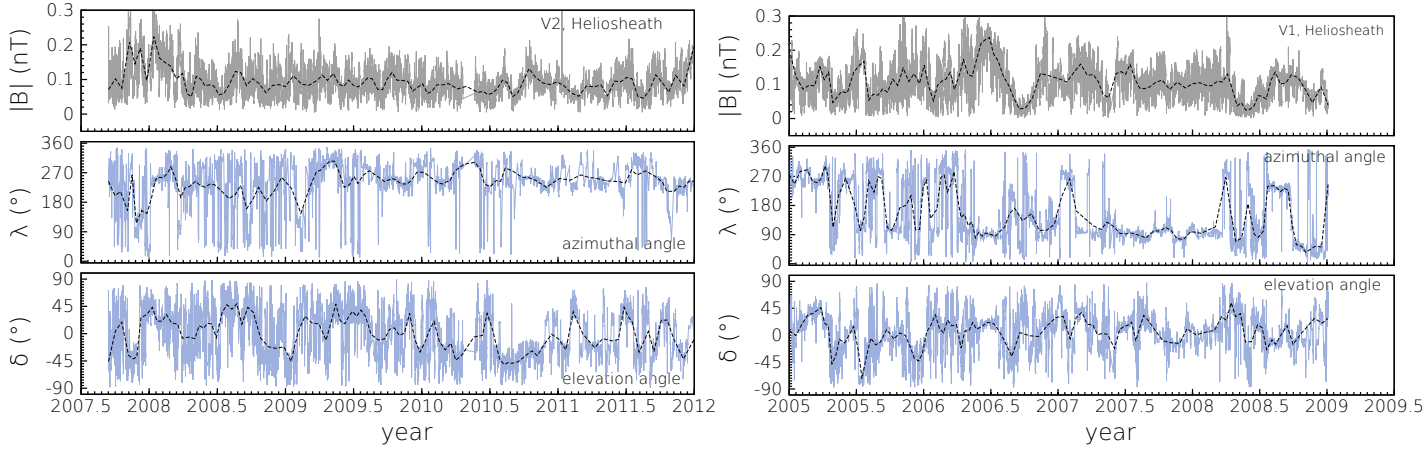

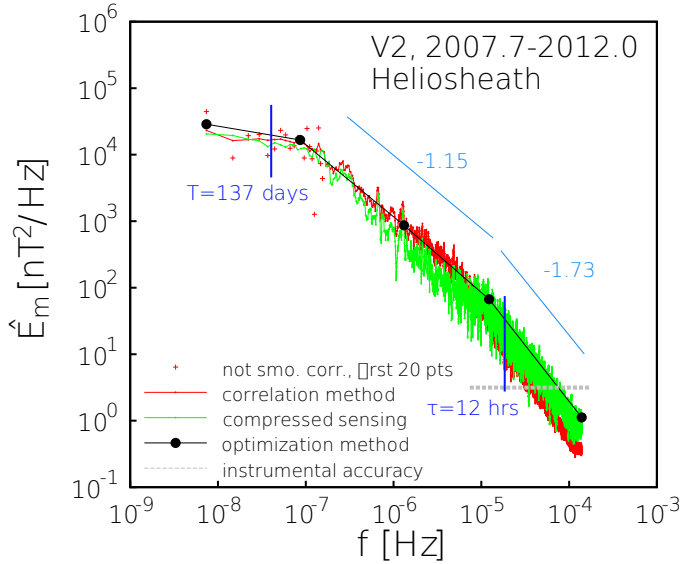

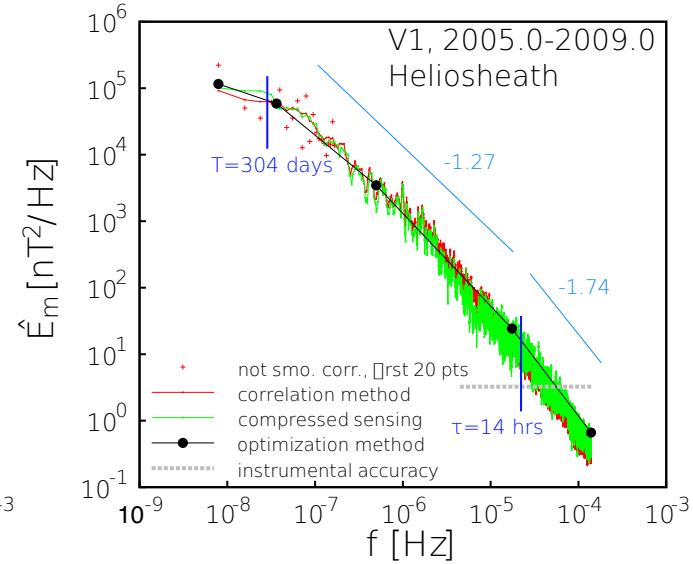

Final considerations and future development

- Spectra computation: it is possible to obtain good spectral estimation from incomplete data even when missing points are many (we tested 4 methods on synthetic sets with 30%-95% of gaps, and spectral exponents $\alpha \in [1, 3]$). Linear interpolation+correlations: loss of energy in the high frequency range, good estimate of the low-freq range. Compress sensing: only few frequency are caught, introduces some noise, provides a good estimate of slopes for the hi-freq range. Iterative procedure: it is able to represent the true spectrum with a piecewise linear model.
- Heliosheath magnetic spectra: the instrumental accuracy is enough to observe up to 10^{-4} Hz. A change in spectral slope is observed at about $f = 10^{-5}$ Hz (1 day), where a turbulent cascade seem to start, $\alpha = 1.75$. At lower frequencies the scaling exponent is about $\alpha = 1.2$. The integral scale increases as the distance from the sun. In early periods the sun rotation ($T \approx 28$ days) is still seen, while the later source for low-freq (T $O(100)$ days) oscillations is not known [Burlaga et al. JGR 2014]. 4-year spectra from V2 and V1 show differences in the low-freq range, V1 spectrum being steeper, with a bigger integral scale.
- Heliosheath plasma velocity spectra: the data accuracy highly limits the observable frequency range.
- Future work:
  - Improve the velocity spectra (at least for $f < 10^{-5}$) by using hi-res data
  - Investigate on the nature of turbulence in HS, role of CRs and the presence of magnetic bubbles
  - Compare results from V1 and V2 data

Optimization method via genetic algorithm

The procedure aims at estimating the error given by the interpolation method. The inversion problem (back from **AA** to **A**) does not have a unique solution. Anyway, convergence to the correct result can be obtained under some restrictions:

- physical underlying process has quasi-random phases (e.g. turbulence) and "simple" continuous spectrum
- Voyagers-like gap distributions (gaps and signal independent)
- data has a sufficient number of points (convergence is always better in the hi-freq. range: better statistics)

Low-freq range: linear method is very close to correct result→ easy to check convergence.
Each control point is free to move inside its band.

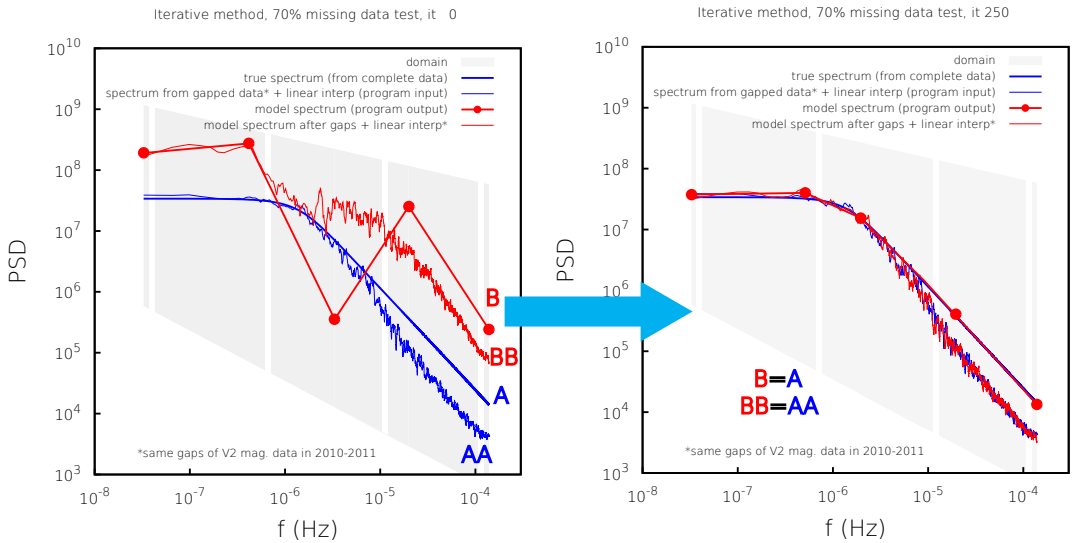

1. Program input: gapped data → interpolation → computation of **AA**
   (true spectrum **A** is unknown, it is the target)
2. Start with a random shape of **B** → IFFT with random phases → gaps + interpolation → compute **BB**
3. Compute the difference **BB**-**AA**, to be minimized
4. Move the control points of **B** and iterate until **BB**=**AA** . Now **B**=**A**

Synthetic sets with 95% of missing data

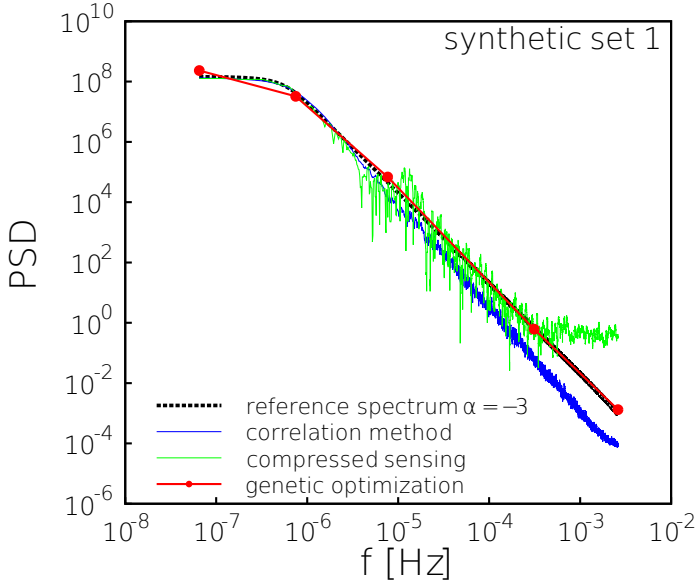

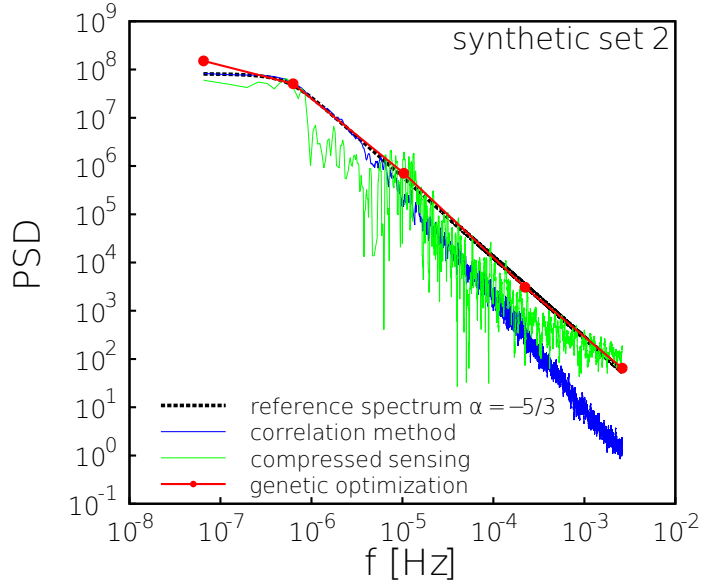

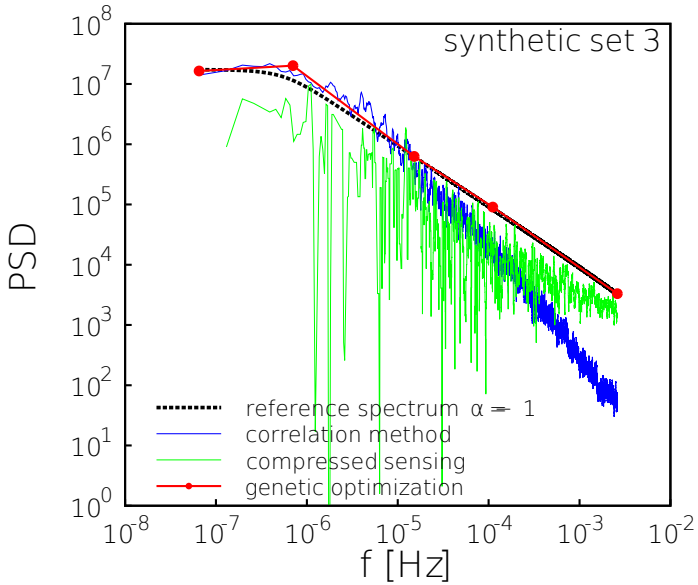

Hi-resolution data ($\Delta t = 192$ s, $n_{tot} = 80000$). Same gaps of V2 plasma data in the period 2007-2008 (95% missing data)

$E_{3D}(n/n_0) = \frac{(n/n_0)^\beta}{1+(n/n_0)^{\alpha+\beta}}$

- set 1 $\rightarrow \beta = 2$, $\alpha = 3$, $k_0 = 10$
- set 2 $\rightarrow \beta = 2$, $\alpha = 5/3$, $k_0 = 10$
- set 3 $\rightarrow \beta = 2$, $\alpha = 1$, $k_0 = 10$

Compressed sensing

- Given $y = Ax$, where $x \in \mathbb{R}^n$, $A \in \mathbb{R}^{m \times n}$, with $m < n$, compressed sensing states how to reconstruct x from the compressed signal y, given A and provided that x is *sparse* (i.e., has few non-zero components)[4]
- Such reconstruction is possible if the matrix A fulfills some conditions. It has been proved that partial (= some rows are missing) Fourier matrices are *good* matrices for this purpose[5]
- Voyager 2 data:
  y = available time series with gaps ($\rightarrow$ compressed)
  x = unknown frequency vector, which is assumed to be sparse ($\rightarrow$ few frequencies are significant)
- Used reconstruction method:
  SPGL1 solver for Basis Pursuit Denoise
  minimize $||x||_1$ subject to $||Ax - y||_2 < \sigma$

[4] Donoho, IEEE TIT, 2006
[5] Rahut 2010

G.B. Rybicki &W.H. Press prediction

- Minimum variance prediction (interpolation):

  $\boldsymbol{y} = \boldsymbol{s} + \boldsymbol{n}$ irreg. spaced vector data with errors $\boldsymbol{n}$

  $s^* = \sum_{i=1}^{M} d_{*i} y_i + x_*$ s^* =true value at a particular point

  $\hat{s^*} = \mathbf{S}^T[\mathbf{S} + \mathbf{N}]^{-1}\mathbf{y}$ $\hat{s^*}$ =min. variance estimate for s^*

  Assuming the process stationary:

  $S_{ij} = \langle s_i s_j \rangle = f(t_i - t_j)$ is the correlation matrix, estimated from data

  $N_{ii} = \langle n_i^2 \rangle$ is the error diagonal matrix $n_i \to \infty$ in "new" points

  The min. variance estimation is not, however, a typical realization of the underlying process.

- Minimum variance prediction + Gaussian process

  To obtain a typical realization, a Gaussian process is added to the min. var. estimate:

  $s_* = u_* + \hat{s_*}$

  If realizations constrained to data are desired:

  $\boldsymbol{u} = \boldsymbol{V} diag(\lambda_1^{1/2}, ..., \lambda_M^{1/2})\boldsymbol{r}$ where

  $\lambda_i = eig(\boldsymbol{Q}), \quad \boldsymbol{Q} = [\boldsymbol{S}^{-1} + \boldsymbol{N}^{-1}]^{-1}, \quad \boldsymbol{r} = rand(\mu = 0, \sigma^2 = 1)$

Spectra of solar wind at 5 AU

Voyager 2 data, 1979 DOY 1-180

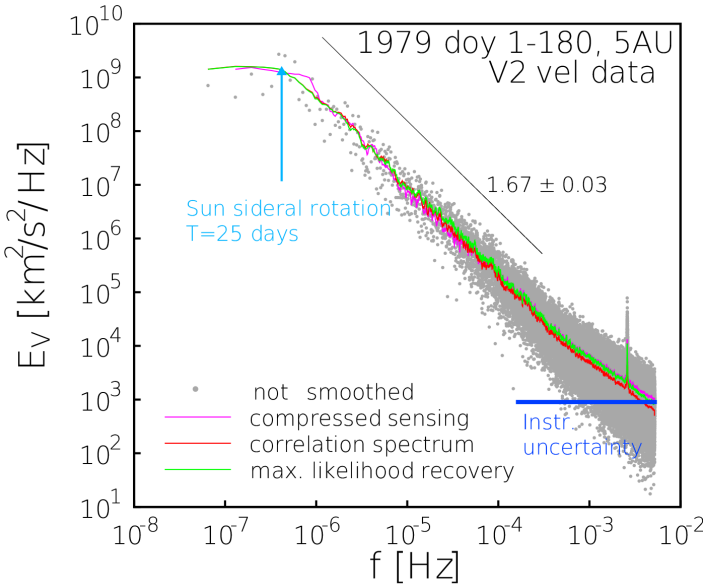

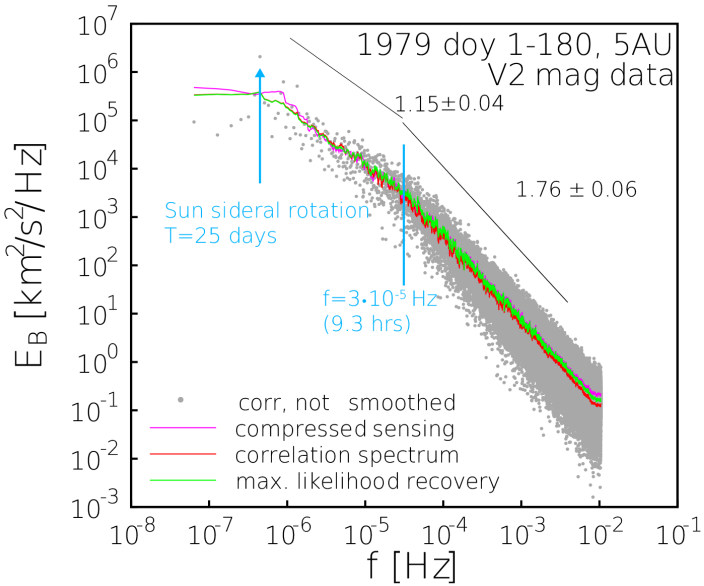

Velocity field:

- Integral scale related to the sun rotation, $T \approx 25$ days, Taylor miscoscale $\tau \approx 1$ h
- Spectral slope in the inertial range is close to the Kolmogorov value
- Influence of instrumental accuracy for $f > 4 \cdot 10^{-4}$ Hz ($1\sigma = 2$ km/s)
- Peak at $f = 2.6 \cdot 10^{-3}$ Hz is instrumental-related

Magnetic field:

- A change in slope occurs at $f \approx 3 \cdot 10^{-5}$ Hz
- Flatter spectrum for $f < 3 \cdot 10^{-5}$ Hz $\rightarrow$ big-scale Alfven waves
- For $f > 3 \cdot 10^{-5}$ Hz the spectral slope is higher than the Kolmogorov value